Available online at www.sciencedirect.com
ScienceDirect
Journal of Hazardous Materials 153 (2008) 1093–1102
Journal of Hazardous Materials
www.elsevier.com/locate/jhazmat

Atmospheric concentrations, dry deposition and air–soil exchange of polycyclic aromatic hydrocarbons (PAHs) in an industrial region in Turkey

Ayse Bozlaker, Aysen Muezzinoglu, Mustafa Odabasi *

Department of Environmental Engineering, Faculty of Engineering, Dokuz Eylul University, Kaynaklar Campus, Buca 35160, Izmir, Turkey

Received 4 May 2007; received in revised form 18 September 2007; accepted 18 September 2007
Available online 21 September 2007

Abstract

Concurrent ambient air and dry deposition samples were collected during two sampling periods at the Aliaga industrial region in Izmir, Turkey. $\sum_{15}$-PAH (particulate + gas) concentrations ranged between 7.3 and 44.8 ng m^{-3} (average ± S.D., 25.2 ± 8.8 ng m^{-3}) and 10.2–71.9 ng m^{-3} (44.1 ± 16.6 ng m^{-3}) in summer and winter, respectively. Winter/summer individual ambient PAH concentration ratios ranged between 0.8 (acenaphthene) and 6.6 (benz[*a*]anthracene) indicating that wintertime concentrations were affected by residential heating emissions. In contrast to the ambient concentrations, $\sum_{15}$-PAH particle dry deposition fluxes were higher in summer (5792 ± 3516 ng m^{-2} day^{-1}, average ± S.D.) than in winter (2650 ± 1829 ng m^{-2} day^{-1}), probably due to large particles from enhanced re-suspension of polluted soil particles and road dust. Average overall dry deposition velocity of PAHs calculated using the dry deposition fluxes and particle-phase concentrations was 2.9 ± 3.5 cm s^{-1}. $\sum_{15}$-PAH concentrations in soils taken from 50 points in the area ranged between 11 and 4628 μg kg^{-1} in dry weight. The spatial distribution of these concentrations indicated that the urban Aliaga, steel plants, the petroleum refinery, and the petrochemical plant are the major Σ_{15}-PAH sources in the area. Fugacity calculations in air and soil showed that the soil acts as a secondary source to the atmosphere for low molecular weight PAHs in summer and as a sink for the higher molecular weight ones in summer and winter.

Keywords: Atmospheric PAHs; Dry deposition flux; Deposition velocity; Soil–air partitioning; Fugacity ratio

1. Introduction

Polycyclic aromatic hydrocarbons (PAHs) are ubiquitous environmental pollutants generated primarily during the incomplete combustion of organic materials (e.g. coal, oil, petrol, and wood). Emissions from anthropogenic activities predominate, but some PAHs in the environment originate from natural sources such as open burning, natural losses or seeps of petroleum or coal deposits, and volcanic activities. Major anthropogenic sources of PAHs include residential heating, coal gasification and liquefying plants, carbon black, coal-tar pitch and asphalt production, coke and aluminum production, catalytic cracking towers and related activities in petroleum refineries, and motor vehicle exhaust [1].

PAHs are found in the ambient air in gas-phase and as sorbed to aerosols. The fate, transport and removal of PAHs from the atmosphere by dry and wet deposition processes are strongly influenced by their gas/particle partitioning. Atmospheric deposition is a major source for PAHs in soil. Direct and indirect methods are used to measure particle-phase dry deposition flux. In the direct method, a surrogate surface is used while in the indirect method measured ambient concentrations are multiplied by an assumed or modeled deposition velocity to determine the dry deposition flux [2]. Deposition velocity is affected by the meteorological parameters, physical properties of the particle (i.e., size, shape and density), and the type and roughness characteristics of the receptor surface [3]. The selection of an appropriate deposition velocity is crucial since it may introduce large uncertainties in the calculation of dry deposition fluxes.

Once deposited, PAHs tend to accumulate in soil for a long period of time and they are subject to various partitioning, degradation and transport processes depending on their physical–chemical properties and microbiological

* Corresponding author. Tel.: +90 232 4127122; fax: +90 232 4530922.
E-mail address: mustafa.odabasi@deu.edu.tr (M. Odabasi).

0304-3894/$ – see front matter © 2007 Elsevier B.V. All rights reserved.
doi:10.1016/j.jhazmat.2007.09.064

degradability. Considering their large reservoir in soils, soil–air exchange is an important diffusive process affecting the fate and transport of PAHs into the environment. The direction and magnitude of the diffusion gradient is determined by their respective concentrations in air and soil, and by the soil–air equilibrium partition coefficient (K_{SA}) [4]. K_{SA} values and soil–air equilibrium status for various semivolatile organic compounds (SOCs) have been calculated previously [4–11]. However, there has been limited investigation on soil–air partition coefficients and fugacities of PAHs [4,12].

The objectives of this study were (1) to measure the ambient air concentrations of PAHs at a heavily polluted industrial area in Turkey, (2) to measure their particle-phase dry deposition fluxes and to determine their deposition velocities, and (3) to determine the spatial variation of PAH concentrations in soil and to investigate their soil–air exchange.

2. Experimental

2.1. Sample collection

Sampling was performed at a site located at the Horozgedigi village in the Aliaga industrial region, ~50 km north of the metropolitan city of Izmir, Turkey. The site is located in the vicinity of main pollutant sources including a large petroleum refinery and a petrochemicals complex, iron smelters with scrap iron storage and classification sites, steel rolling mills, a very dense transportation activity of scrap iron trucks, heavy road and rail traffic, ship dismantling areas, busy ports with scrap iron dockyards, and nearby agricultural and residential areas (Fig. 1).

Concurrent ambient air and dry deposition samples were collected during two sampling programs carried out between August 2–17, 2004 and March 20–April 5, 2005. During the sampling programs, 28 samples (14 samples in summer and 14 samples in winter) were collected. Average sampling duration was ~24 h. Both sampling periods coincided with dry weather days. Meteorological data was provided from a meteorological station located at the sampling site. Sampling information and meteorological data are summarized in Table 1. Average air temperatures were 9.3 and 24.4 °C for winter and summer sampling periods, respectively. Wind speed ranged between 1.7–9.4 and 1.5–5.5 m s^{-1} during the winter and summer sampling periods, respectively. Generally northerly winds (WNW, NW) prevailed (except for 4 days of SE winds) during the sampling programs.

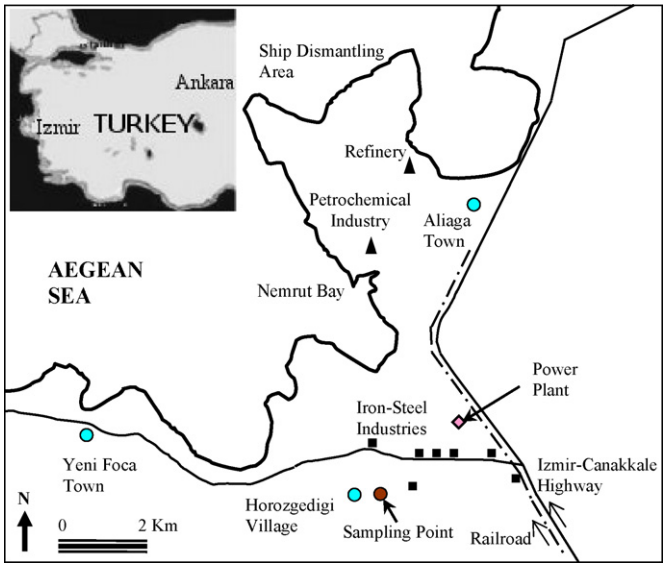

Fig. 1. General layout of the study area.

Air samples were collected using a modified high-volume sampler, Model GPS-11 (Thermo-Andersen Inc.). Particles were collected on 10.5 cm diameter quartz filters while the gas-phase compounds were collected using a modified cartridge containing XAD-2 resin placed between polyurethane foam (PUF) plugs. Average sampling volumes were 257 ± 22 and 309 ± 21 m^3 for the summer and winter periods, respectively.

The particle dry deposition flux was measured concurrently using a smooth deposition plate (22 cm × 7.5 cm) with a sharp leading edge (<10°), mounted on a wind vane [2]. Glass fiber filter (GFF) sheets mounted with cellulose acetate strips on the plates were used to collect the deposited particles. The dimensions of the deposition surface of the GFF sheet were 5.5 cm × 12.5 cm. Five plates and sheets with a total collection area of 344 cm^2 were used for sampling.

Prior to sampling, quartz and GFF filters were baked at 450 °C overnight to remove any organic matter residual. Then, they were allowed to cool to room temperature in a desiccator. PUF cartridges were cleaned by Soxhlet extraction using a dichloromethane (DCM)/petroleum ether (PE) mixture (20:80) for 24 h, were dried in an oven at 70 °C, and were stored in glass jars capped with Teflon-lined lids. After sampling, PS-1 filters and PUF cartridges were stored at −20 °C in their containers.

Seven soil samples were taken around the air-sampling site during the sampling campaigns. Additional soil samples were taken from 50 different points in the study area in March 2006 to determine the spatial distribution of PAH contamination that can be related to the local sources. Approximately, 0.5–1 kg of soil samples were taken from the top 5 cm of the soil after removal of the large stones and pieces of vegetation. Samples were wrapped with aluminum foil, put into airtight plastic bags, and stored in a freezer.

2.2. Sample preparation and analysis

Extraction and analysis of samples were carried out in accordance with the literature [13–15]. Briefly, collected samples were separately Soxhlet extracted using 20:80 mixture of DCM:PE for 24 h. Prior to extraction, all samples were spiked with PAH surrogate standards to monitor analytical recovery efficiencies. The volume of extracts was reduced and was transferred into hexane using a rotary evaporator and a high-purity N_2 stream. After volume reduction to 2 ml by a gentle flow of nitrogen, the samples were cleaned up on an alumina–silicic acid column containing 3 g of silicic acid (deactivated with 3% water) and 2 g of alumina (deactivated with 6% water). The column was pre-washed with 20 ml of DCM followed by 20 ml of

Table 1
Summary of sampling information and meteorological data

Sampling date	Sampling duration (min)	Air temperature (°C)	Wind speed ($m\,s^{-1}$)	Prevailing wind direction	RH (%)
08/02–03/2004	1460	24.1	3.9	NW	62
08/03–04/2004	1426	23.9	2.4	WNW	66
08/04–05/2004	1412	24.4	1.8	WNW	61
08/05–06/2004	1490	24.1	1.9	WNW	70
08/06-07/2004	1423	25.1	1.5	W	64
08/07–08/2004	1301	24.1	2.5	WNW	76
08/08–09/2004	1394	24.3	3.3	WNW	71
08/09–10/2004	1316	24.7	2.5	WNW	67
08/10–11/2004	1607	23.3	2.9	WNW	72
08/11–12/2004	1302	23.4	4.1	NW	66
08/12–13/2004	1441	24.3	3.1	WNW	60
08/13–14/2004	1476	24.8	1.7	WNW	56
08/14–15/2004	1528	26.4	1.6	SSE	57
08/15–16/2004	1419	24.4	5.5	WNW	68
Sampling period average ± S.D.	1428	24.4 ± 0.8	2.8 ± 1.1	WNW	66 ± 6
Seasonal average ± S.D.[a]		23.8 ± 1.6	3.4 ± 1.4	WNW	62 ± 9
03/20–21/2005	1333	6.4	4.0	WNW	64
03/21–22/2005	1360	7.9	2.7	NW	46
03/22–23/2005	1433	8.0	3.1	NW	30
03/23–24/2005	1455	8.5	2.5	NW	37
03/24–25/2005	1384	9.9	2.3	NW	36
03/25–26/2005	1502	11.0	1.7	SSE	54
03/27–28/2005	1383	16.1	6.7	SE	60
03/28–29/2005	1340	16.2	6.1	SE	62
03/29–30/2005	1418	13.4	2.1	WNW	74
03/30–31/2005	1452	12.1	2.7	NW	77
04/01–02/2005	1243	5.0	9.4	NW	58
04/02–03/2005	1466	4.8	8.2	WNW	56
04/03–04/2005	1361	4.8	5.6	WNW	50
04/04–05/2005	1454	6.6	4.7	WNW	45
Sampling period average ± S.D.	1399	9.3 ± 3.9	4.4 ± 2.5	NW	54 ± 14
Seasonal average ± S.D.[b]		7.8 ± 3.7	3.7 ± 2.1	NW	44 ± 31

[a] Refers to the average of a period from 06.01.2004 to 08.31.2004.
[b] Refers to the average of a period from 12.01.2004 to 04.05.2005.

PE. The sample in 2 ml of hexane was added to the top of the column and PAHs were eluted with 20 ml of DCM. After solvent exchange into hexane, the final sample volume was adjusted to 1 ml by nitrogen blow-down.

The soil samples were sieved through a 0.5 mm mesh sieve to remove large particles and organic debris. Soil moisture content was determined by weighing sub-samples of soils before and after drying at 103 °C in an oven for 24 h, and organic matter content was determined by loss on ignition in a muffle furnace at 600 °C for 4 h using Standard Methods of 2540-B and 2540-E, respectively [16]. Method 2540-E has been commonly used because it offers an approximation of the amount of organic matter present in the solid fraction [17,18]. For the PAH analysis, 15 g of samples were spiked with 0.5 ml PAH surrogate standards and were soaked in 50 ml of a 1:1 acetone:hexane mixture overnight. Then, they were ultrasonically extracted for 30 min. For the concentration and clean up steps, the same procedures used for the air and dry deposition samples were applied.

All extracts were analyzed for 15 PAHs including acenaphthene (ACT), fluorene (FLN), phenanthrene (PHE), anthracene (ANT), carbazole (CRB), fluoranthene (FL), pyrene (PY), benz[*a*]anthracene (BaA), chrysene (CHR), benz[*b*]fluoranthene (BbF), benz[*k*]fluoranthene (BkF), benz[*a*]pyrene (BaP), indeno[1,2,3-*cd*]pyrene (IcdP), dibenz[*a,h*]anthracene (DahA), and benzo[*g,h,i*]perylene (BghiP) with a gas chromatograph (GC) (Agilent 6890N) equipped with a mass selective detector (Agilent 5973 inert MSD). A capillary column (HP5-ms, 30 m, 0.25 mm, 0.25 μm) was used. The initial oven temperature was held at 50 °C for 1 min, was raised to 200 °C at 25 °C min^{-1} and from 200 to 300 °C at 8 °C min^{-1}, and was held for 5.5 min. The injector, ion source, and quadrupole temperatures were 295, 300, and 180 °C, respectively. High purity helium was used as the carrier gas at constant flow mode (1.5 ml min^{-1}, 45 cm s^{-1} linear velocity). The MSD was run in selected ion-monitoring mode. Compounds were identified on the basis of their retention times, target and qualifier ions and were quantified using the internal standard calibration procedure [19].

2.3. Quality control

Average recoveries of surrogate standards were 59 ± 16% for acenaphthene-d_{10}, 87 ± 15% for phenanthrene-d_{10}, 84 ± 10% for chrysene-d_{12}, and 81 ± 21% for perlylene-d_{12} for all air and deposition samples (n = 90). For soil samples, average surrogate recoveries were 50 ± 13% for acenaphthene-d_{10}, 68 ± 12% for

phenanthrene-d_{10}, 72 ± 10% for chrysene-d_{12}, and 75 ± 14% for perlylene-d_{12} for all samples (n = 61).

Instrumental detection limits (IDLs) were determined from linear extrapolation from the lowest standard in calibration curve using the area of a peak having a signal/noise ratio of 3. The quantifiable PAH amount was approximately 0.15 pg for 1 μl injection. Blank PUF cartridges and filters were routinely placed in the field to determine if there was any contamination during sample handling and preparation. For the compounds detected in blanks the limit of detection (LOD) of the method was defined as the mean blank mass plus three standard deviations. Instrumental detection limit was used for the compounds that were not detected in blanks. Sample quantities exceeding the LOD were quantified and blank-corrected by subtracting the mean blank amount from the sample amount.

PAH compounds from benzo[*b*]fluoranthene to benzo[*g,h,i*]perylene were generally not detected in blanks. Phenanthrene had the largest amounts found in blanks with an average of 88.1 ± 28.3 ng for PUFs, 64.8 ± 16.4 ng for PS-1 filters and 53.4 ± 2.9 ng for dry deposition filters. Blank amounts for PUFs, PS-1 filters, and dry deposition filters were 3 ± 2%, 9 ± 12%, 26 ± 12% of the sample amounts, respectively. Generally, PAHs from benzo[*b*]fluoranthene to benzo[*g,h,i*]perylene were not detected in soil blanks (n = 4). Phenanthrene had the largest amounts found in blanks with an average of 44.3 ± 2.5 ng. Average blank amounts were 7 ± 12% of the amounts found in soil samples.

Six levels of calibration standards (0.04, 0.4, 1.0, 4.0, 6.0, and 10.0 μg ml^{-1}) were used to calibrate the GC/MS system. In every case, the r^2 of the calibration curve was ≥0.999. System performance was verified by the analysis of the mid-point calibration standard for every 24 h during the analysis period.

3. Results and discussion

3.1. Ambient air concentrations

$\sum_{15}$-PAH (particulate + gas) concentrations ranged between 7.3–44.8 ng m^{-3} (average ± S.D., 25.2 ± 8.8 ng m^{-3}) and 10.2–71.9 ng m^{-3} (average ± S.D., 44.1 ± 16.6 ng m^{-3}) in summer and winter, respectively (Table 2). Winter/summer PAH concentration ratios ranged between 0.8 (acenaphthene) and 6.6 (benz[*a*]anthracene). Higher PAH concentrations observed during winter were probably due to the increasing emissions from residential heating. Different ratios for individual compounds indicate that residential heating emissions create a different ambient PAH profile compared to summertime. Similar increases in winter PAH concentrations were recently reported [20–25]. Concentrations measured in this study were within the range of previously reported values in other urban and industrial sites around the world (Table 2). Total $\sum_{15}$-PAH concentrations measured in this study are considerably lower than those reported by Odabasi et al. [14] for urban Chicago, by Fang et al. [26] for industrial and urban sites in Taiwan, and by Possanzini et al. [27] for urban Rome. However, the PAH levels determined in this study are similar to those reported by Ohura et al. [21] for industrial sites in Fuji and Shimizu,

Table 2
Ambient PAH concentrations (particle + gas-phase, ng m^{-3}) measured in this study and previously reported for urban and industrial sites

	Taiwan[a]		Rome[b]	Fuji[c]		Shimizu[c]		Heraklion[d]	Athens[e]	Baltimore[f]	Chicago[g]	Aliaga[h]	
	Industrial	Urban		S	W	S	W		S	S		S	W
ACT	202.2	143.1	59.2	6.4	2.9	3.5	2.5				76.9	1.6	1.3
FLN	138.8	95.7	18.9	9.8	5.8	5.6	4.7	5.2	1.4	4.1	74.8	4.1	5.2
PHE	94.2	63.2	78.2	26.3	12.6	17.3	10.1	20.0	6.5	12.6	200.3	13.4	17.6
ANT	163.6	109.1	6.1	0.4	0.9	0.3	0.3	3.3	1.0	0.3	14.1	0.5	1.5
CRB											6.1	0.3	0.2
FL	84.4	58.9	21.5	4.6	3.2	1.9	1.6	4.9	3.0	3.6	44.1	2.9	5.5
PY	81.6	54.5	16.8	3.0	2.9	1.5	1.2	6.6	2.1	2.3	24.6	2.0	4.3
BaA	14.2	20.3	1.8	0.1	1.0	0.0	0.4	1.1	0.3	0.1	2.1	0.1	0.9
CHR	50.7	34.3	4.4	0.4	1.6	0.1	0.9			0.1	3.6	0.7	3.0
BbF	12.8	9.1		0.5	1.5	0.1	1.1	1.5			2.3	0.3	1.3
BkF	14.5	12.6		0.2	0.7	0.1	0.4	1.8			1.9	0.2	1.0
BaP	9.0	6.4	2.7	0.2	1.1	0.1	0.5	1.2	0.2	0.1	1.6	0.1	0.7
IcdP	3.9	4.2	1.6	0.2	1.1	0.1	0.6	2.5	0.5	0.3	1.2	0.1	0.9
DahA	4.3	2.9		0.0	0.1	0.0	0.1	0.1	0.1	0.0		0.1	0.3
BghiP	6.7	5.5	2.9	0.3	1.3	0.1	0.6	3.4	0.4	0.3	1.1	0.2	1.1
Total	880.9	619.8	211.2	52.5	36.6	30.7	25.1	51.5	15.4	23.8	428.7	26.5	44.8

S, summer; W, winter.
[a] Fang et al. [26] (summer–winter).
[b] Possanzini et al. [27] (Urban site, annual).
[c] Ohura et al. [21] (Industrial sites).
[d] Tsapakis and Stephanou [28] (Urban site, annual).
[e] Mandalakis et al. [30] (Urban site).
[f] Dachs et al. [29] (Urban/industrial site, summer).
[g] Odabasi et al. [14] (Urban site, summer–fall).
[h] This study.

Tsapakis and Stephanou [28] for urban Heraklion, Dachs et al. [29] for urban/industrial Baltimore, and Mandalakis et al. [30] for urban Athens. The emissions from major industries may affect the sampling site if the winds are from N and NE (Fig. 1). However, during the sampling programs the prevailing winds were WNW and NW and probably therefore, relatively low concentrations were measured.

The contribution of PAH compounds to the total atmospheric concentrations decreased with increasing molecular weight. Phenanthrene, fluorene, fluoranthene, and pyrene accounted for 51, 15, 11, and 7% of $\sum_{15}$-PAHs in summer period, respectively while they were 39, 12, 12, and 10% of $\sum_{15}$-PAHs in winter period. These contributions were similar to those reported by Odabasi et al. [14], Gevao et al. [25], and Possanzini et al. [27].

The following equation was used to assess the effect of meteorological parameters (temperature, wind speed and direction) on PAH concentrations [31]:

$$C_t = m_1 T + m_2 U + m_3 \cos \mathrm{WD} + b \quad (1)$$

where C_t is the total (gas+particle phase) PAH concentration (ng m^{-3}), T is the mean temperature (°C), U is the wind speed (m s^{-1}), WD is the predominant wind direction (deg) during the sampling period, and m_1, m_2, m_3, and b are the regression parameters.

For the full dataset, temperature, wind speed and wind direction together accounted for 26% (acenaphthene) to 80% (benzo[*a*]anthracene) of the variability in the atmospheric PAH concentrations (Table 3). The correlations and m_1 values were statistically significant for all PAHs ($p < 0.05$–0.1) except for acenaphthene. Generally negative m_1 values were obtained for PAHs indicated that their concentrations increased with decreasing temperature. This was probably due to increased PAH emissions from combustion sources like residential heating with decreased ambient temperature. For most of the compounds, m_2 had positive values and they were statistically significant for eight compounds indicating that advection was also a controlling parameter for the atmospheric PAHs. m_3 values were generally positive and statistically significant for seven PAHs (acenaphthene through pyrene). Negative values point southerly directions for build-up of high concentrations while positive cosine values are associated with northerly winds. Different directions observed for individual compounds may be due to their different sources affecting the sampling site. Multiple linear regression (MLR) analysis was repeated for the two subsets of data (winter and summer samples). The results were similar for winter samples to those obtained from the full dataset. However, m_1 values were generally insignificant for the summer sampling period probably due to the observed narrow temperature range (23.3–26.4 °C).

Table 3
Summary of regression parameters for Eq. (1)

PAHs	m_1	m_2	m_3	r^2	n
ACT	0.012	−0.034	0.554[a]	0.26[b]	27
FLN	−0.134[a]	−0.371[a]	1.199[b]	0.48[a]	28
PHE	−0.366[a]	0.230	6.010[a]	0.47[a]	28
ANT	−0.060[a]	0.095[a]	0.612[a]	0.75[a]	28
CRB	0.007[b]	0.036[a]	0.222[a]	0.46[a]	28
FL	−0.148[a]	0.013	1.628[b]	0.47[a]	28
PY	−0.134[a]	0.336[a]	1.149[b]	0.64[a]	28
BaA	−0.052[a]	−0.001	0.052	0.80[a]	28
CHR	−0.144[a]	0.192[b]	0.156	0.66[a]	28
BbF	−0.069[a]	−0.066	0.044	0.58[a]	27
BkF	−0.052[a]	0.058[b]	0.128	0.77[a]	27
BaP	−0.043[a]	−0.047[b]	−0.094	0.67[a]	28
IcdP	−0.055[a]	0.006	−0.090	0.69[a]	28
DahA	−0.015[a]	0.037[a]	0.050	0.64[a]	28
BghiP	−0.063[a]	0.032	−0.038	0.68[a]	28

[a] $p < 0.05$.
[b] $p < 0.10$.

Results of MLR analysis indicated that meteorological parameters have significant effect on the ambient PAH concentrations. Meteorological parameters (i.e., temperature, wind speed and direction) measured during the sampling programs of the present study were not significantly different than the seasonal averages (Table 1). This suggests that the measured ambient PAH concentrations during the sampling periods are representative for the winter and summer seasons.

3.2. Particle phase dry deposition fluxes and velocities

$\sum_{15}$-PAH particle dry deposition fluxes were 5792 ± 3516 ng m^{-2} day^{-1} (average ± S.D.) and 2650 ± 1829 ng m^{-2} day^{-1} in summer and winter, respectively (Table 4). No previous measurement of PAH dry deposition in this area was available for comparison. Deposition fluxes measured in this study were within the range of values reported previously elsewhere (Table 4). The particle-phase PAH dry deposition fluxes measured by Franz et al. [32] for rural Lake Michigan were considerably lower. However, fluxes measured in this study were lower than those reported for urban Chicago [2,32], and for the industrial, urban and rural areas in Taiwan [26]. Unlike the ambient PAH concentrations, dry deposition fluxes were higher in summer than in winter. Due to the prevailing Mediterranean climate in this area, the soil is dry with a weaker vegetation cover in summer. Since large particles dominate the atmospheric dry deposition, higher summer fluxes can be attributed to larger particles from enhanced re-suspension of polluted soil particles and road dust.

Low molecular weight PAHs had a larger fraction in the dry deposition flux similar to their large contribution to the atmospheric concentrations (Table 4). Phenanthrene, fluorene, acenaphthene, and fluoranthene accounted for 45, 21, 8, and 5% of $\sum_{15}$-PAH fluxes in summer, while phenanthrene, fluorene, chrysene, and fluoranthene accounted for 36, 13, 11, and 8% of $\sum_{15}$-PAH fluxes in winter, respectively.

Measured dry deposition fluxes were plotted against the atmospheric concentrations to investigate their relationship. All compounds analyzed and all samples collected in summer ($n = 175$) and winter ($n = 159$) sampling periods were included. The correlations between the fluxes and the concentrations were statistically significant for summer ($r^2 = 0.23$, $p < 0.01$) and winter periods ($r^2 = 0.49$, $p < 0.01$). Particle phase dry deposition velocities (V_d, cm s^{-1}) of PAHs were calculated using the dry deposition fluxes measured with dry deposition plates and

Table 4
Particle-phase dry deposition fluxes (average ± S.D., ng m^{-2} day^{-1}) of individual PAHs determined in this study and reported previously

PAHs	Taiwan[a]			Chicago[b]	Chicago[c]	Lake Michigan[c]	Aliaga[d]	
							Summer	Winter
ACT	860	900	560	3300	120	12	703 ± 412	240 ± 4
FLN	3,470	2,480	2,300	4,200	110	5	1801 ± 1135	645 ± 121
PHE	1,160	640	780	47,100	1,560	60	3788 ± 911	1784 ± 285
ANT	2,370	1,450	1,660	1,600	190	8	181 ± 121	124 ± 35
CRB				1,900			75 ± 39	10 ± 7
FL	1,620	1,840	1,090	25,500	2,710	106	459 ± 157	403 ± 186
PY	690	210	460	22,900	2,240	77	435 ± 189	343 ± 153
BaA	140	330	80	7,000	1,090	25	124 ± 91	162 ± 109
CHR	950	800	600	9,100	1,880	94	236 ± 110	563 ± 435
BbF	1,720	1,120	1,140	9,600	2,910[e]	114[e]	123 ± 38	195 ± 137
BkF	1,340	1,090	880	8,600			114 ± 70	131 ± 78
BaP	350	550	230	7,700	1,100	49	97 ± 89	105 ± 71
IcdP	2,040	1,850	1,340	6,300	770	31	100 ± 65	48 ± 37
DahA	3,190	1,180	2,100		330	17	54 ± 32	51 ± 42
BghiP	2,820	1,900	1,850	5,400	990	48	153 ± 180	137 ± 98
Total	22,720	16,340	15,070	160,200	16,000	646	5792 ± 3516	2650 ± 1829

[a] Fang et al. [26] (industrial, urban and rural sites, respectively; summer–winter period; obtained using a model).
[b] Odabasi et al. [2] (urban site; summer–fall period; with greased dry deposition plates).
[c] Franz et al. [32] (urban and rural sites respectively; summer–winter and summer periods, respectively; with greased dry deposition plates).
[d] This study.
[e] Benzo[*b*]fluoranthene+ benzo[*k*]fluoranthene.

atmospheric particle phase concentrations. V_d ranged between 0.7 ± 0.2 cm s^{-1} (benz[*b*]fluoranthene) and 11.5 ± 2.7 cm s^{-1} (acenaphthene) with an average of 3.6 ± 3.6 cm s^{-1} in summer, and between 0.07 ± 0.04 cm s^{-1} (indeno[1,2,3-*cd*]pyrene) and 9.1 ± 2.5 cm s^{-1} (fluorene) with an overall average of 1.4 ± 2.4 cm s^{-1} in winter. The seasonal differences in deposition velocities are probably due to the variations of particle size distribution and the meteorological conditions (i.e., wind speed, ambient air temperature, and atmospheric stability).

Using greased dry deposition plates, Franz et al. [32] have reported that deposition velocities for the individual PAHs were between 0.4–2.1 and 1.0–3.7 cm s^{-1} in summer and winter in Chicago, respectively. Odabasi et al. [2] calculated V_d values between 4.3 and 9.8 cm s^{-1} with an average of 6.7 cm s^{-1} in urban Chicago for a summer/fall period. Similarly, Vardar et al. [33] have reported the mean overall dry deposition velocity of PAHs as 4.5 cm s^{-1} for winter period in Chicago. The overall average deposition velocities of individual PAHs are illustrated in Fig. 2. The overall average deposition velocity for PAHs was 2.9 ± 3.5 cm s^{-1}. This value is higher than the values typically assumed to calculate PAH dry deposition, however, it agrees well with the values determined using similar measurement techniques for dry deposition fluxes.

The overall dry deposition velocity for individual PAHs generally decreased with increasing molecular weight. The average overall dry deposition velocity for PAHs with molecular weights between 154 and 202 was 4.2 cm s^{-1} and for PAHs with molecular weights between 228 and 276 it was 0.6 cm s^{-1}. The overall dry deposition velocity for individual PAHs were well correlated with molecular weight ($r^2 = 0.67$, $p < 0.01$) (Fig. 2). This decrease in deposition velocity with increasing molecular weight is supported by other experimental studies which have indicated that a greater fraction of the higher molecular weight PAHs are associated with fine particles relative to the lower molecular weight compounds [34–36]. A similar decrease in deposition velocity with increasing molecular weight was previously reported for PAHs [2,32,33,37].

3.3. PAH concentrations in soil and air–soil exchange

The soil $\sum_{15}$-PAH concentrations measured in this study ranged between 11 and 4628 μg kg^{-1} dry weight (dry wt) and they were within the range of previously reported values (Table 5). $\sum_{15}$-PAH concentrations in soil reported by Zhang et al. [38] for the urban and rural areas in Hong Kong and Nadal et al. [18] for the industrial and unpolluted areas in Spain are lower

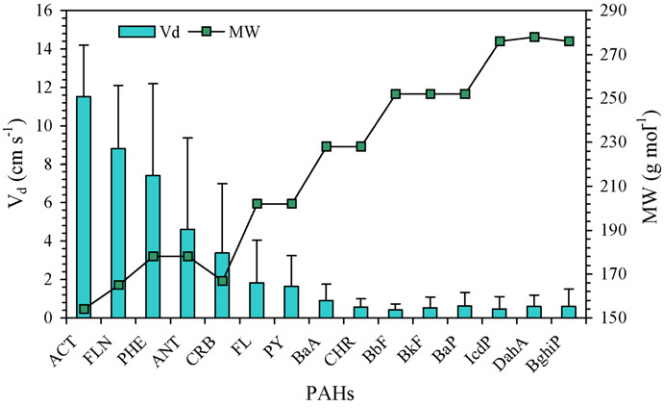

Fig. 2. Overall particulate dry deposition velocities of PAHs measured in this study.

Table 5
Minimum, maximum and average concentrations of PAHs in soil (μg kg^{-1} dry wt) (mean ± S.D.) measured in this study and reported previously

PAHs	Hong Kong [a]		France [b]			Spain [c]		Aliaga, Turkey (this study)		
	Urban	Rural	Industrial	Urban	Remote	Industrial	Residential	Min.	Max.	Air-sampling site
ACT	0.5	nd	36	nd	2.5	1	5	nd	28.7	2.5 ± 1.0
FLN	4.6	2.4	9	5	4.7	23	13	nd	59.7	3.7 ± 0.7
PHE	16.7	2.1	254	132	38	131	114	1.2	647.6	29.9 ± 6.9
ANT	3.6	1.1	10	17	3.9	51	17	0.1	130.2	4.3 ± 1.1
CRB								0.3	28.9	0.6 ± 0.3
FL	28	8.8	834	292	144	180	97	2.3	504.3	34.0 ± 9.5
PY	27.1	3.3	581	219	160	159	96	1.5	506.7	32.1 ± 9.7
BaA	9	1.5	244	127	30.9	137	68	0.4	315.9	22.3 ± 8.0
CHR	16.2	0.4	319	196	31.7	120	68	1.9	651.6	54.2 ± 20.4
BbF	26.7[d]	1.5[d]	313	161	24.7	9	2	0.9	360.8	31.4 ± 10.3
BkF			139	73	8.9	9	47	0.6	225.6	19.1 ± 5.0
BaP	9.9	3.4	249	126	14.4	100	56	0.4	288.4	18.6 ± 5.5
IcdP	8.3	0.04	145	116	9.8	16	60	0.5	208.8	22.3 ± 6.9
DahA			21	16	0.4	6	21	0.2	195.5	23.4 ± 13.3
BghiP	9.8	2.2	239	166	21.1	41	40	0.7	474.7	43.0 ± 19.8
Total	160.3	26.6	3393	1646	495	983	704	11.0	4628	341.3 ± 109.7

[a] Zhang et al. [38].
[b] Motelay-Massei et al. [41].
[c] Nadal et al. [18].
[d] BbF + BkF.

than the values obtained in this study, while other investigations have reported similar or higher $\sum_{15}$-PAH values.

Spatial distribution of $\sum_{15}$-PAH concentrations in soil was mapped out by MapInfo Professional (Version 7.5) with Vertical Mapper (Version 3.0) (Fig. 3). The highest $\sum_{15}$-PAH concentrations were measured around the Aliaga town, steel plants, the petroleum refinery, and the petrochemical plant indicating that these are the major PAH sources in the area (Fig. 3).

Seasonal soil PAH concentrations were only measured in the air sampling site. Results indicated that there were not large seasonal variations in soil PAH concentrations for all compounds (summer/winter concentration ratio was between 0.75 and 1.4).

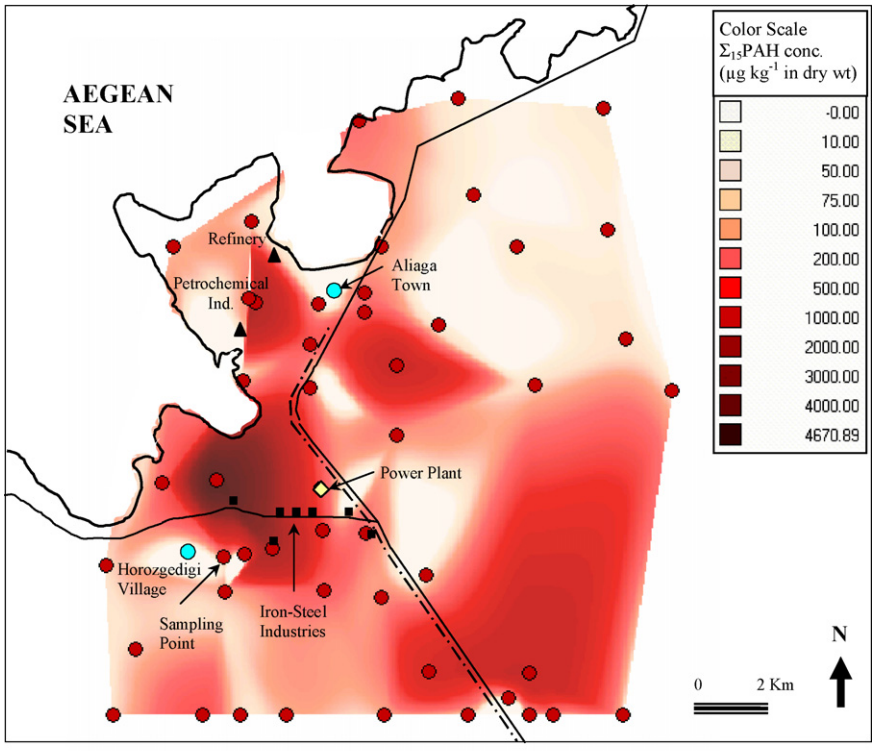

Fig. 3. Spatial variation of soil PAH concentrations. Filled circles show the soil sampling sites.

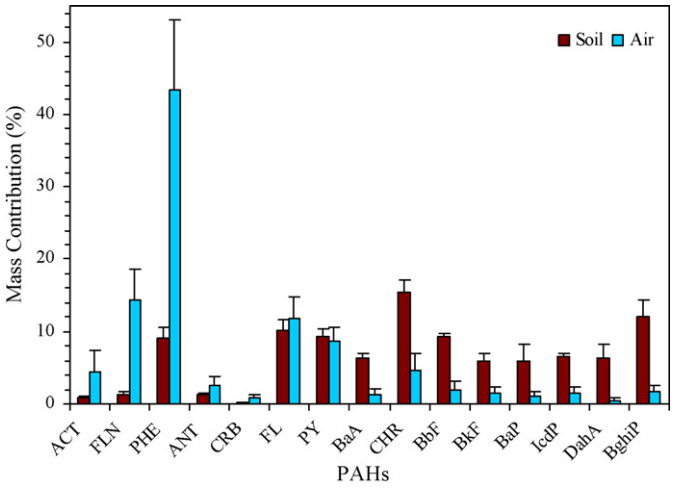

Fig. 4. PAH profiles in ambient air and soil.

The average soil $\sum_{15}$-PAH concentration in the air sampling site was relatively low ($341.3 \pm 109.7\ \mu g\ kg^{-1}$ dry wt) and this site was not affected significantly by the major sources in the area. Thus, the relatively low ambient concentrations measured at the air-sampling site can be attributed to its location and the prevailing wind direction.

Unlike the air samples the PAH profile in soil was dominated by high molecular weight compounds (Fig. 4). Chrysene, benzo[*g,h,i*]perylene, fluoranthene, and pyrene accounted for 16, 13, 10, and 9% of the $\sum_{15}$-PAHs, respectively. Since the sampling point is relatively close to the local sources, this can be explained by the 4–6-ring PAHs being deposited more easily close to the point sources than the lower molecular weight ones which are mainly in gaseous form and capable of long-range transport [18]. Although the $\sum_{15}$-PAH concentrations of ambient air were dominated by three-ring PAHs, they accounted for only 12% of the total PAHs in soil. The difference in air and soil PAH profiles is also due to their different partitioning behaviors (i.e., low molecular weight compounds have relatively low soil–air partition coefficients). Volatilization from the previously polluted surfaces as a result of enhanced ambient air temperature and wind speed was suggested to be the dominant loss mechanism especially for the low molecular weight PAHs [12,39]. Soil PAH profiles were also variable for different sites. This was probably due to the sources having different profiles affecting those sites. Variable distances from the sources may also have resulted in a change of PAH profiles during the transport.

Fugacity is a measure of chemical potential or partial pressure of a chemical in a particular medium that controls the transfer of chemicals between media. Chemicals try to establish an equal fugacity (equilibrium) in the soil–air system [8]. The equilibrium partitioning of a chemical between air and soil is described by the dimensionless soil–air partition coefficient, K_{SA} as follows:

$$K_{SA} = \frac{C_S \rho_S}{C_A} \tag{2}$$

where C_S is the soil concentration ($ng\ kg^{-1}$, dry wt), ρ_S is the density of soil solids ($kg\ m^{-3}$), and C_A is the gas-phase air concentration ($ng\ m^{-3}$). If the system is not at equilibrium the use of the term K_{SA} is incorrect and the values obtained from Eq. (2) are defined as soil–air quotients (Q_{SA}) [6].

K_{SA} is dependent on temperature, humidity and the chemical and soil properties [6]. Partitioning of persistent organic pollutants to soil occurs via absorption to the organic carbon fraction. The octanol–air partition coefficient (K_{OA}) is a key descriptor of chemical partitioning between the atmosphere and organic phases [9]. Hippelein and McLachlan [4] formulated a linear relationship that relates the K_{SA} to K_{OA} and to the organic carbon fraction of the soil as follows:

$$K_{SA} = 0.411 \rho_S \phi_{OC} K_{OA} \tag{3}$$

where ρ_S is the density of the soil solids ($kg\ l^{-1}$) and ϕ_{OC} is the fraction of organic carbon on a dry soil basis. The factor 0.411 improves the correlation between the K_{SA} and K_{OA} [4,5]. Temperature dependent K_{OA} values can be measured directly for compounds of interest, while K_{SA} is soil-specific.

K_{SA} can also be expressed as a ratio of the fugacity capacity (Z-value; $mol\ m^{-3}\ Pa^{-1}$) for soil and air:

$$K_{SA} = \frac{Z_{Soil}}{Z_{Air}} \tag{4}$$

The following equation can be used to calculate Z_{air} values:

$$Z_{Air} = \frac{1}{(RT)} \tag{5}$$

where R is the universal gas constant ($8.314\ Pa\ m^3\ mol^{-1}\ K^{-1}$) and T is absolute temperature (K). Combining Eqs. (3)–(5), Z_{soil} can be expressed as:

$$Z_{Soil} = \frac{0.411 \rho_S \phi_{OC} K_{OA}}{(RT)} \tag{6}$$

Concentration of compounds (C_i, $mol\ m^{-3}$) can be converted to fugacity (f_i, Pa) in medium i using the relationship as follows:

$$f_i = \frac{C_i}{Z_i} \tag{7}$$

When performing this conversion for soil, it was assumed that the fugacity capacity of soil is entirely due to the organic carbon fraction [5,8].

Concurrent air and soil concentrations are used to assess the fugacity gradients of individual PAHs between the soil–air interfaces. The soil–air fugacity ratio (f_S/f_A) > 1 indicates that the soil is a source with net re-volatilization of compounds from soil while values < 1 indicate that the soil is a sink and net gas-phase deposition occurs from air to soil.

The fugacity ratios were calculated only at the air-sampling site since both air and soil concentrations were available. The average water and organic matter contents of soil samples were 7.2 and 8.8% (in dry sample), respectively. It was assumed that the organic matter fraction is 1.5 times the organic carbon fraction and the density of soil solids was $2.0\ g\ cm^{-3}$ for all calculations. K_{OA} values of the individual PAHs used for Eq. (3) were calculated as a function of temperature using the regression parameters recently reported by Odabasi et al. [19,40]. A

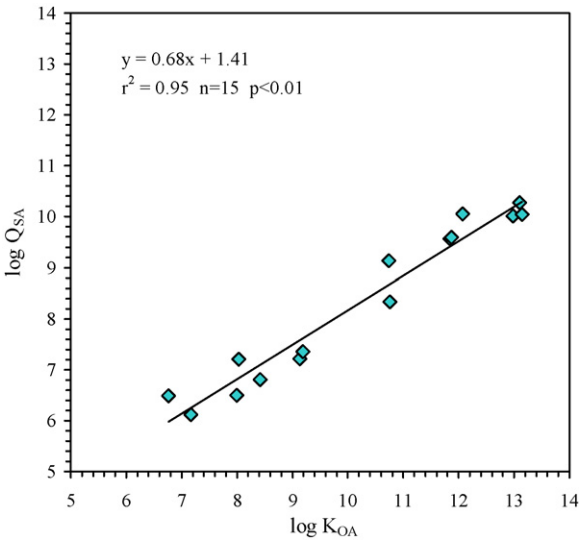

Fig. 5. $\log Q_{SA}$ vs. $\log K_{OA}$.

statistically significant correlation was found between $\log Q_{SA}$ and $\log K_{OA}$ ($r^2 = 0.95$, $p < 0.01$) indicating that the octanol is a good surrogate for soil organic matter (Fig. 5).

For a system in equilibrium, f_S/f_A value is approximately equal to 1 [9,12]. Assuming a 15% R.S.D. in C_A, C_S, and K_{OA} (used to calculate K_{SA}) [6,19,40], a propagation of the errors that are associated with the calculation indicated that the equilibrium is represented by an f_S/f_A of 1.0 ± 0.26 (i.e., a range of 0.74–1.26). Generally, the fugacity ratios of all compounds fell outside this uncertainty range and it can be concluded that for these compounds the soil and ambient air are not in equilibrium. For some samples (overall, 11% of the data set) the fugacity ratios for fluorene through pyrene were in the equilibrium range. The contaminated soil acts as a secondary source to the atmosphere for low molecular weight, three-ring PAHs for both seasons (Fig. 6). Similarly, Cousins and Jones [12] have reported fugacity ratios greater than 1 for the low molecular weight PAHs. Soil–air partitioning of the medium volatility compounds (carbazole-benz[*a*]anthracene) was more sensitive to the seasonal air concentration and ambient air temperature changes than the compounds having lower and higher volatility

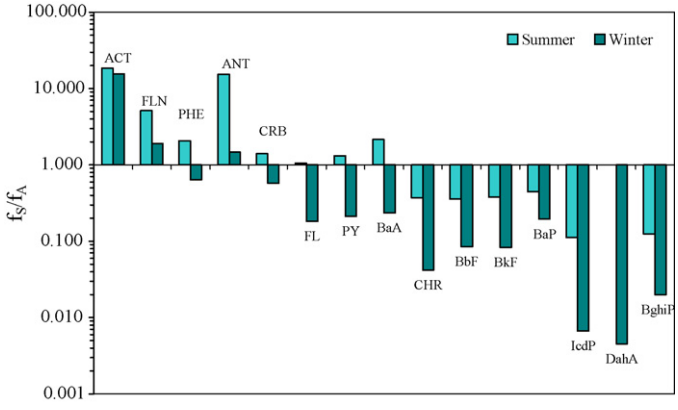

Fig. 6. Calculated average soil/air fugacity ratios for individual PAHs.

as indicated by their shift from volatilization to deposition from summer to winter. Once deposited, the heavier molecular weight PAHs with high K_{SA} values tend to accumulate in soil for long periods. Thus, the soil acted as a sink for these compounds for both seasons (Fig. 6).

Acknowledgments

This study was supported in part by the scientific research fund of Dokuz Eylul University (project no: 03.KB.FEN.101). We would like to thank Faruk Dincer (Dokuz Eylul University) for his assistance in air sampling. We are also grateful to ENKA power station in Aliaga, Izmir for allowing the use of their air pollution measurement station and meteorological data generated at this site.

References

[1] R. Dabestani, I.N. Ivanov, A compilation of physical, spectroscopic and photophysical properties of polycyclic aromatic hydrocarbons, Photochem. Photobiol. 70 (1999) 10–34.
[2] M. Odabasi, A. Sofuoglu, N. Vardar, Y. Tasdemir, T.M. Holsen, Measurement of dry deposition and air-water exchange of polycyclic aromatic hydrocarbons with the water surface sampler, Environ. Sci. Technol. 33 (1999) 426–434.
[3] D. Golomb, E. Barry, G. Fisher, P. Varanusupakul, M. Koleda, T. Rooney, Atmospheric deposition of polycyclic aromatic hydrocarbons near New England coastal waters, Atmos. Environ. 35 (2001) 6245–6258.
[4] M. Hippelein, M.S. McLachlan, Soil/air partitioning of semivolatile organic compounds. 1. Method development and influence of physical–chemical properties, Environ. Sci. Technol. 32 (1998) 310–316.
[5] T.F. Bidleman, A.D. Leone, Soil–air exchange of organochlorine pesticides in the Southern United States, Environ. Pollut. 128 (2004) 49–57.
[6] S.N. Meijer, M. Shoeib, L.M.M. Jantunen, K.C. Jones, T. Harner, Air–soil exchange of organochlorine pesticides in agricultural soils 1. Field measurements using a novel in situ sampling device, Environ. Sci. Technol. 37 (2003) 1292–1299.
[7] S.N. Meijer, M. Shoeib, K.C. Jones, T. Harner, Air–soil exchange of organochlorine pesticides in agricultural soils. 2. Laboratory measurements of the soil–air partition coefficients, Environ. Sci. Technol. 37 (2003) 1300–1305.
[8] S.N. Meijer, T. Harner, P.A. Helm, C.J. Halsall, A.E. Johnston, K.C. Jones, Polychlorinated naphthalenes in U.K. soils: time trends, markers of source, and equilibrium status, Environ. Sci. Technol. 35 (2001) 4205–4213.
[9] T. Harner, N.J.L. Green, K.C. Jones, Measurements of octanol–air partition coefficients for PCDD/Fs: a tool in assessing air–soil equilibrium status, Environ. Sci. Technol. 34 (2000) 3109–3114.
[10] M. Hippelein, M.S. McLachlan, Soil/air partitioning of semivolatile organic compounds. 2. Influence of temperature and relative humidity, Environ. Sci. Technol. 34 (2000) 3521–3526.
[11] I.T. Cousins, M.S. McLachlan, K.C. Jones, Lack of an aging effect on the soil–air partitioning of polychlorinated biphenyls, Environ. Sci. Technol. 32 (1998) 2734–2740.
[12] I.T. Cousins, K.C. Jones, Air–soil exchange of semi-volatile organic compounds (SOCs) in the UK, Environ. Pollut. 102 (1998) 105–118.
[13] A. Sofuoglu, M. Odabasi, Y. Tasdemir, N.R. Khalili, T.M. Holsen, Temperature dependence of gas-phase polycyclic aromatic hydrocarbon and organochlorine pesticide concentrations in Chicago air, Atmos. Environ. 35 (2001) 6503–6510.
[14] M. Odabasi, N. Vardar, A. Sofuoglu, Y. Tasdemir, T.M. Holsen, Polycyclic aromatic hydrocarbons (PAHs) in Chicago air, Sci. Total Environ. 227 (1999) 57–67.

[15] T. Harner, T.F. Bidleman, Octanol–air partition coefficient for describing particle/gas partitioning of aromatic compounds in urban air, Environ. Sci. Technol. 32 (1998) 1494–1502.
[16] A.D. Eaton, L.S. Clesceri, E.W. Rice, A.E. Greenberg, Standard Methods for the Examination of Water and Wastewater, 21st Centennial ed., American Public Health Association (APHA), American Water Works Association (AWWA), Water Environment Federation (WEF), 2005.
[17] C. Backe, I.T. Cousins, P. Larsson, PCB in soils and estimated soil–air exchange fluxes of selected PCB congeners in the south of Sweden, Environ. Pollut. 128 (2004) 59–72.
[18] M. Nadal, M. Schuhmacher, J.L. Domingo, Levels of PAHs in soil and vegetation samples from Tarragona County Spain, Environ. Pollut. 132 (2004) 1–11.
[19] M. Odabasi, E. Cetin, A. Sofuoglu, Determination of octanol–air partition coefficients and supercooled liquid vapor pressures of PAHs as a function of temperature: application to gas/particle partitioning in an urban atmosphere, Atmos. Environ. 40 (2006) 6615–6625.
[20] J. Schnelle-Kreis, M. Sklorz, A. Peters, J. Cyrys, R. Zimmermann, Analysis of particle associated semi-volatile aromatic and aliphatic hydrocarbons in urban particulate matter on a daily basis, Atmos. Environ. 39 (2005) 7702–7714.
[21] T. Ohura, T. Amagai, M. Fusaya, H. Matsushita, Spatial distributions and profiles of atmospheric polycyclic aromatic hydrocarbons in two industrial cities in Japan, Environ. Sci. Technol. 38 (2004) 49–55.
[22] S.S. Park, Y.J. Kim, C.H. Kang, Atmospheric polycyclic aromatic hydrocarbons in Seoul, Korea, Atmos. Environ. 36 (2002) 2917–2924.
[23] S.Y. Bae, S.M. Yi, Y.P. Kim, Temporal and spatial variations of the particle size distribution of PAHs and their dry deposition fluxes in Korea, Atmos. Environ. 36 (2002) 5491–5500.
[24] G. Kiss, Z. Varga-Puchony, B. Tolnai, B. Varga, A. Gelencser, Z. Krivacsy, J. Hlavay, The seasonal changes in the concentration of polycyclic aromatic hydrocarbons in precipitation and aerosol near Lake Balaton, Hungary, Environ. Pollut. 114 (2001) 55–61.
[25] B. Gevao, J. Hamilton-Taylor, K.C. Jones, Polychlorinated biphenyl and polycyclic aromatic hydrocarbon deposition to and exchange at the air–water interface of Esthwaite Water, a small lake in Cumbria, UK, Environ. Pollut. 102 (1998) 63–75.
[26] G.C. Fang, K.F. Chang, C. Lu, H. Bai, Estimation of PAHs dry deposition and BaP toxic equivalency factors (TEFs) study at Urban, Industry Park and rural sampling sites in central Taiwan, Taichung, Chemosphere 55 (2004) 787–796.
[27] M. Possanzini, V. Di Palo, P. Gigliucci, M.C.T. Sciano, A. Cecinato, Determination of phase-distributed PAH in Rome ambient air by denuder/GC–MS method, Atmos. Environ. 38 (2004) 1727–1734.
[28] M. Tsapakis, E.G. Stephanou, Occurrence of gaseous and particle polycyclic aromatic hydrocarbons in the urban atmosphere: study of sources and ambient temperature effect on the gas/particle concentration and distribution, Environ. Pollut. 133 (2005) 147–156.
[29] J. Dachs, T.R. Glenn IV., C.L. Gigliotti, P. Brunciak, L.A. Totten, E.D. Nelson, T.P. Franz, S.J. Eisenreich, Processes driving the short-term variability of PAHs in the Baltimore and northern Chesapeake Bay atmosphere, USA, Atmos. Environ. 36 (2002) 2281–2295.
[30] M. Mandalakis, M. Tsapakis, A. Tsoga, E.G. Stephanou, Gas-particle concentrations and distribution of aliphatic hydrocarbons, PAHs, PCBs and PCDD/Fs in the atmosphere of Athens (Greece), Atmos. Environ. 36 (2002) 4023–4035.
[31] A. Sofuoglu, E. Cetin, S.S. Bozacioglu, G.D. Sener, M. Odabasi, Short-term variation in ambient concentrations and gas-particle partitioning of organochlorine pesticides in Izmir, Turkey, Atmos. Environ. 38 (2004) 4483–4493.
[32] T.P. Franz, S.J. Eisenreich, T.M. Holsen, Dry deposition of particulate polychlorinated biphenyls and polycyclic aromatic hydrocarbons to Lake Michigan, Environ. Sci. Technol. 32 (1998) 3681–3688.
[33] N. Vardar, M. Odabasi, T.M. Holsen, Particulate dry deposition and overall deposition velocities of polycyclic aromatic hydrocarbons, J. Environ. Eng. 128 (2002) 269–274.
[34] J.O. Allen, N.M. Dookeran, K.A. Smith, A.D. Sarofim, K. Taghizadeh, A.L. Lafleur, Measurement of polycyclic aromatic hydrocarbons associated with size-segregated atmospheric aerosols in Massachusetts, Environ. Sci. Technol. 30 (1996) 1023–1031.
[35] G. Kiss, Z. Varga-Puchony, G. Rohrbacher, J. Hlavay, Distribution of polycyclic aromatic hydrocarbons on atmospheric particles of different sizes, Atmos. Res. 46 (1998) 253–261.
[36] H. Kaupp, M.S. McLahlan, Atmospheric particle size distributions of polychlorinated dibenzo-*p*-dioxins and dibenzofurans (PCDD/Fs) and polycyclic aromatic hydrocarbons (PAHs) and their implications for wet and dry deposition, Atmos. Environ. 33 (1999) 85–95.
[37] A.S. Shannigrahi, T. Fukushima, N. Ozaki, Comparison of different methods for measuring dry deposition fluxes of particulate matter and polycyclic aromatic hydrocarbons (PAHs) in the ambient air, Atmos. Environ. 39 (2005) 653–662.
[38] H.B. Zhang, Y.M. Luo, M.H. Wong, Q.G. Zhao, G.L. Zhang, Distributions and concentrations of PAHs in Hong Kong soils, Environ. Pollut. 141 (2006) 107–114.
[39] I.T. Cousins, A.J. Beck, K.C. Jones, A review of the process involved in the exchange of semi-volatile organic compounds (SVOC) across the air–soil interface, Sci. Total Environ. 228 (1999) 5–24.
[40] M. Odabasi, B. Cetin, A. Sofuoglu, Henry's law constant, octanol–air partition coefficient and supercooled liquid vapor pressure of carbazole as a function of temperature: application to gas/particle partitioning in the atmosphere, Chemosphere 62 (2006) 1087–1096.
[41] A. Motelay-Massei, D. Ollivon, B. Garban, M.J. Teil, M. Blanchard, M. Chevreuil, Distribution and spatial trends of PAHs and PCBs in soils in the Seine River basin, France, Chemosphere 55 (2004) 555–565.